

## RECONSTRUCTION OF POLYGONAL CYLINDRICAL TARGETS WITH CURVED SURFACES FROM THEIR RCS VALUES

Hiroshi SHIRAI, Yoshinori HIRAMATSU, and Masashi SUZUKI  
Graduate School of Science and Engineering, Chuo University  
1-13-27 Kasuga, Bunkyo, Tokyo 112-8551 Japan  
E-mail: shirai@m.ieice.org

### 1. Introduction

Target identification is one of the important topics for remote sensing and next generation radar technologies, and various methods, which are mainly based on the signal processing techniques or numerical methods, have been proposed previously for this purpose. Radar Cross Section (RCS) is one of the fundamental values to evaluate the equivalent size of the scatterer, and it is known that RCS changes according to the scatterer's shape[1, 2]. Authors have already been studied that high frequency asymptotic techniques such as the Geometrical Theory of Diffraction (GTD)[3] and the Equivalent Source Method (ESM)[4], can be confidently used for analyzing various electromagnetic wave scattering by large polygonal scatterers[5].

Reconstruction algorithm for polygonal cylinder using high frequency techniques, has already been proposed first for the case when the convex cylindrical targets are composed by flat plate facets [6]. This reconstruction algorithm is mainly based on our finding that for polygonal objects, the main contribution to the backscattering arises from the edge diffracted waves at the facet at the specular reflection direction, and each facet size can be estimated by the local RCS maxima and its lobe width. Reconstruction is then made for closed cross-sectional convex objects by simply connecting these facets in order[6]. While this algorithm works well for convex bodies, the order of specular reflection direction may be interchanged when the surface of the scattering body has concave portions. In order to overcome this difficulty for estimating the concave portion of the polygonal targets, we have also utilized the time domain RCS responses at the possible specular reflection directions in the frequency domain. From these time domain data, one can identify the wavefront arrivals, whose delay times can be used for estimating the location of the facets [7].

In the previous works, we assumed that targets are composed by flat metal facets. In this paper, we extend our previous reconstruction algorithm to handle the case when the facets have curved surfaces. The measured and numerically computed monostatic RCS values of half and quarter circular cylinders are used to evaluate our algorithm, and it is found that it works well for predicting flat and curved facets of the metal targets.

### 2. Reconstruction Algorithm

#### 2.1 Polygonal approximation of curved surfaces

In order to evaluate the wave scattering from smooth curved surfaces, it may be natural to approximate the curved surface by polygonal one with many edges. By high frequency asymptotic analysis, it is already known that one can obtain pretty accurate results by polygonal approximation with a few edges for large smooth objects[4].

Figure 1(a) shows a truncated circular cylinder approximated by  $n$ -sided regular polygon, whose cross-sectional area is taken to be the same as that of the original circular cylinder. Monostatic RCS values are computed by the ESM with inclusion up to 4-th multiple edge diffracted waves. When the polygon is rotated, the RCS changes due to the undulated surface, and its maximum variation  $\Delta\sigma$  is shown in Fig.1(b) for  $ka = 22.6$ ,  $kb = 37.7$  ( $k$ : wave number,  $a$ : radius of the original cylinder,  $b$ : axial length of the cylinder). As one expects, the variation

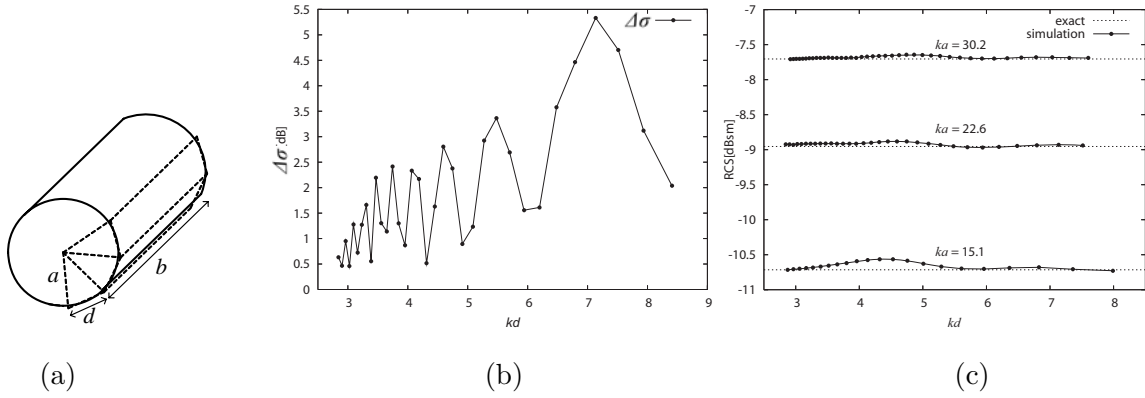


Figure 1: (a) Approximation by regular polygonal cylinder. (b) Maximum variation  $\Delta\sigma$  of polygonal cylinder due to the rotation along the axis.  $ka = 22.6$ ,  $kb = 37.7$ . (c) Angular average RCS value of polygonal cylinders.  $ka = 15.1, 22.6, 30.2$ ,  $kb = 37.7$ .

$\Delta\sigma$  becomes small when the circular surface is approximated by many edges. Angular average RCS values are also computed and plotted in Fig.1(c). From this figure, one observes that the angular average RCS of the polygonal cylinder can predict pretty well that of the original circular cylinder, or equivalently, the radius of the curvature  $a$ .

Figures 2(a) and (b) show the angular RCS variation of half and quarter circular cylinders ( $ka = 25.1, kb = 37.7$ ), respectively. While the solid line denotes the values measured in the anechoic chamber at 24GHz frequency, the dotted line denotes the simulated values for the (equivalent) polygonal cylinder ( $kd = 3.95$ ). Also included is the theoretical RCS ( $-8.50\text{dBsm}$ ) for complete circular cylinder. One can see that the RCS from the curved surface direction, oscillates around this theoretical value, and the measured (simulated) average value from  $0^\circ$  to  $180^\circ$  is  $-8.33$  ( $-8.55$ ) dBsm for half circular cylinder (Fig.2(a)), and the average from  $0^\circ$  to  $90^\circ$  is  $-8.17$  ( $-8.62$ ) dBsm for quarter circular cylinder (Fig.2(b)), respectively. These values are closely matched with the exact one. Accordingly, it may be concluded that the polygonal approximation works well when  $\Delta\sigma$  is less than 2dB.

## 2.2 Reconstruction algorithm for polygonal cylinders with curved surfaces

As seen in Figs.2(a) and (b), there are some differences in the vicinity of the specular reflection direction from a target for angular RCS change. For the return from a flat facet, one observes pretty narrower (pencil beam type) peak at the specular reflection direction, and one can estimate the size of the facet from its local maxima and the lobe width, as we reported in

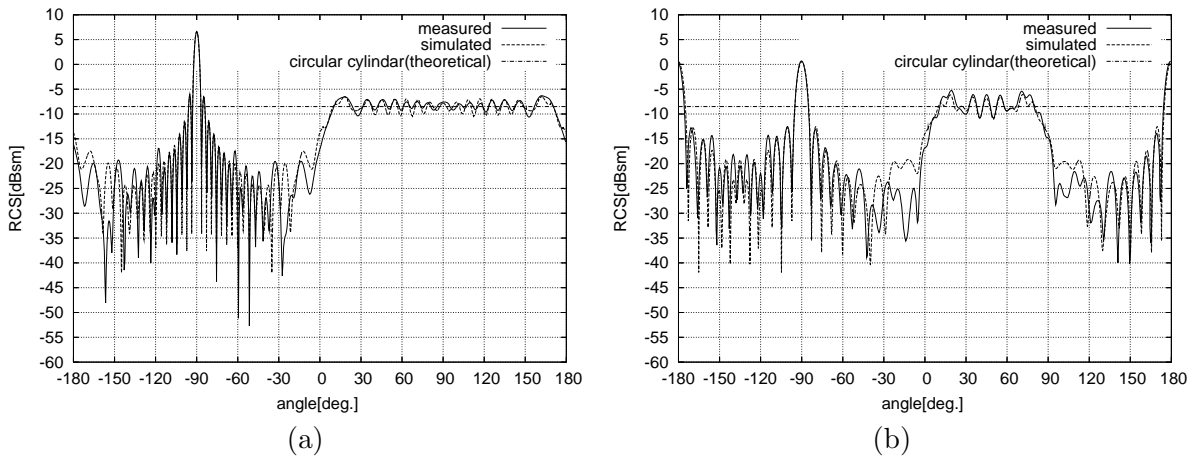


Figure 2: Monostatic RCS change in the angular domain. Frequency: 24GHz, axial length: 75mm,  $ka = 25.1$ ,  $kb = 37.7$ . (a) Half circular cylinder. (b) Quarter circular cylinder.

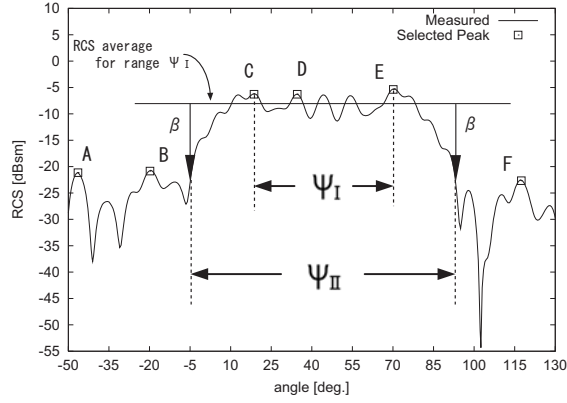


Figure 3: Determination of angular range  $\psi_I, \psi_{II}$  for curved surface

Table 1: Estimation of angular range  $\psi_I, \psi_{II}$ , and the radius of the curvature  $\rho_{II}$ , of the curved surface by  $\beta$  values. (a) Half circular cylinder. (b) Quarter circular cylinder.

(a)			(b)		
$\beta$ [dB]	$\psi_{II}$ [°]	$\rho_{II}$ [mm]	$\beta$ [dB]	$\psi_{II}$ [°]	$\rho_{II}$ [mm]
(true value)	180.0	50.0	(true value)	90.0	50.0
measured			measured		
5	173.5	55.0	5	83.5	58.7
6	175.5	54.4	6	85.0	57.9
7	177.5	54.0	7	88.0	56.3
8	<b>180.0</b>	53.3	8	<b>90.0</b>	55.3
9	182.0	<b>52.8</b>	9	93.0	<b>53.8</b>
simulated			simulated		
5	<b>179.0</b>	<b>48.9</b>	5	87.0	<b>49.5</b>
6	181.6	48.5	6	<b>91.6</b>	48.0
7	183.2	48.1	7	93.3	47.1
8	184.6	47.8	8	94.8	46.5
9	185.8	47.6	9	96.0	46.0

Ref.[6]. For the return from a curved facet, on the other hand, one observes rather broad peak with slight wiggle in the angular range. By considering the above observation, we propose the following reconstruction algorithm:

**Step 1:** From angular monostatic RCS variation, extract the local maxima, and select again local maxima (peaks) from them, as shown in Fig.3.

**Step 2:** If the neighboring peaks change more than 2 dB (like peaks A, B, and F), regard that the peaks are due to the specular reflections from independent flat (straight) facets. Then estimate the size (transverse length  $c$  and axial length  $b$ ) of these facets by the algorithm proposed previously in Ref.[6].

**Step 3:** If not (like peaks C, D, and E), then regard that these neighboring peaks are caused by a curved surface of a facet. Calculate first the average RCS over the angle range  $\psi_I$  from peak C to peak E, then determine the angle range  $\psi_{II}$  of the curved facet at  $\beta$  dB down from the average RCS level. Calculate again for the average RCS over angle  $\psi_{II}$ , and estimate the radius of the curvature  $\rho_{II}$ .

### 3. Reconstructed Results and Discussion

By the above algorithm, we have estimated curved facet dimensions of half and quarter circular cylinders, as shown in Table 1, and Figs.4. Angular range  $\psi_{II}$  can mainly be affected

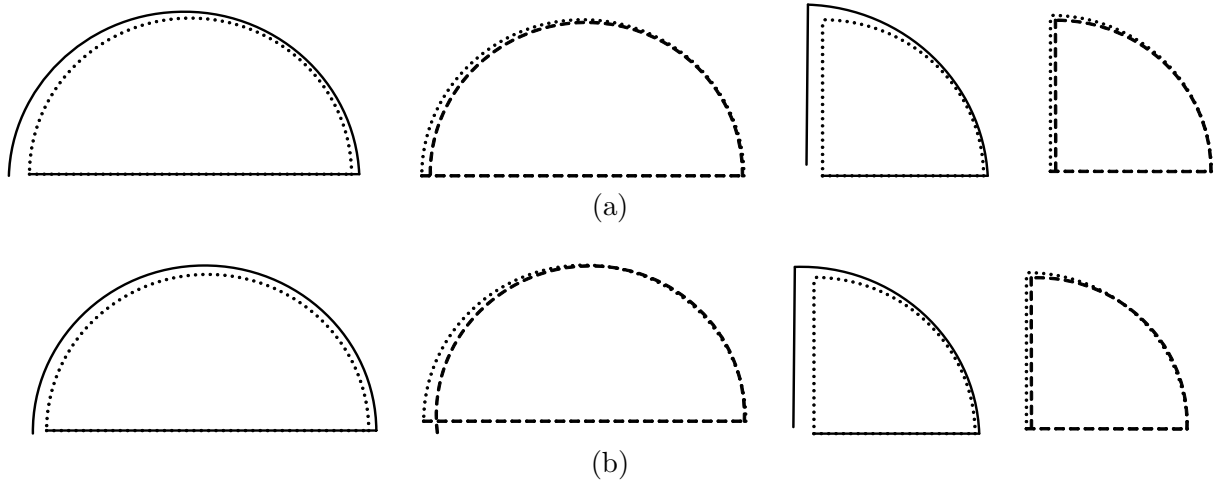


Figure 4: Cross-sectional views of the reconstructed targets. From left to right, these are obtained from the measured data (—), and the numerically simulated data (---) of Fig.2(a) for the half circular cylinder, and Fig.2(b) for the quarter circular cylinder, respectively. Dotted lines are theoretical ones. (a)  $\beta = 6\text{dB}$ . (b)  $\beta = 8\text{dB}$ .

by parameter  $\beta$ . Table 1 shows the estimated angle range  $\psi_{II}$  and the radius of curvature  $\rho_{II}$ . By comparing with the original values,  $\beta$  should be chosen as 6 to 8 dB. Figures 4 show the reconstructed cross-section of half and quarter circular cylinders. Here parameter  $\beta$  is 6 for Fig.4(a) and 8 for Fig.4(b), respectively. Good estimation has been confirmed by these figures.

#### Acknowledgements

This work is partially supported by 2004 Chuo University Personal Research Grant.

#### References

- [1] E. F. Knott: *Radar Cross Section Measurement*, Van Nostrand Reinhold, NY, 1993.
- [2] E. F. Knott, J.F. Shaeffer, and M.T. Tuley: *Radar Cross Section*, 2nd ed., Artech House, Boston, 1993.
- [3] J. B. Keller: "Geometrical theory of diffraction," *J. Opt. Soc. Am.*, **52**(2), pp.116–130, 1962.
- [4] H. Shirai, K. Hongo, and H. Kobayashi: "Diffraction of cylindrical wave by smooth and convex polygonal cylinders," *Trans. of IECE*, **E66**(2), pp.116–123, 1983.
- [5] T. Hayashi, H. Shirai, and H. Sekiguchi: "Plane wave scattering by polygonal cylinders," *IEEJ Technical Report*, **EMT-97-36**, pp.61–66, 1997 (in Japanese).
- [6] K. Ono, H. Shirai, S. Aritake: "Target reconstruction of convex cylindrical scatterers using their monostatic RCS," *IEICE Trans. on Electron.*, **J87-C**(3), pp.296–302, 2004 (in Japanese).
- [7] H. Shirai, S. Suzuki, and K. Ono: "Cylindrical target reconstruction using their frequency and time domain RCS values," *Proc. of ISAP2004*, CDROM, 2004.